



Early treatment response of patients undergoing concurrent chemoradiotherapy for cervical cancer: An evaluation of integrated multi-parameter PET-IVIM MR



Chen Xu^{a,b}, Hongzan Sun^{a,b,*}, Siyao Du^{a,b}, Jun Xin^a

^a Department of Radiology, Shengjing Hospital of China Medical University, Sanhao Street No 36, Heping District, Shenyang, Liaoning, 110004, China

^b Liaoning Provincial Key Laboratory of Medical Imaging, Sanhao Street No 36, Heping District, Shenyang, Liaoning, 110004, China

ARTICLE INFO

Keywords:

Cervical cancer
Integrated PET-MR
Concurrent chemoradiotherapy
Treatment response

ABSTRACT

Purpose: To evaluate the value of integrated multi-parameter positron emission tomography-intravoxel incoherent motion magnetic resonance (PET-IVIM MR) imaging in the assessment of treatment response in patients with cervical cancer treated with concurrent chemoradiotherapy (CCRT).

Materials and methods: A total of 41 patients underwent PET-MR scans before, during (at the end of the third week) and after CCRT were included in this study. The PET-MR imaging parameters were measured on the tumor and the percentage change between the two time points were calculated before and during the treatment. These parameters were used to evaluate treatment response. A combination prediction model was constructed using multivariate logistic regression. European Organization for Research and Treatment of Cancer (EORTC) criteria, measured by the post-therapy (PostTx) PET/MR were used to classify treatment responses: patients were classified into the complete metabolic responder (CMR) group or the non-complete metabolic responders (N-CMR) group. The correlations between PET and IVIM parameters and percentage changes during CCRT were investigated using the Spearman rank correlation.

Results: In all, 13 of 41 (31.7%) patients were defined as N-CMR group. According to constructing multivariate logistic regression, the combination of pre-therapy (Pre-Tx) total metabolic tumor volume (MTV), the percentage changes of the maximum standardized uptake value ($\Delta\text{SUV}_{\text{max}}$) and the mean diffusion-related coefficient ($\Delta\text{D}_{\text{mean}}$) during CCRT had the strongest predictive potentiality (AUC 0.912, $P < 0.05$). In addition, during CCRT the percentage changes in minimum diffusion-related coefficient ($\Delta\text{D}_{\text{min}}$) was correlated with $\Delta\text{SUV}_{\text{max}}$ (Spearman correlation coefficient, $r = 0.338$, $P < 0.05$).

Conclusions: The combination of Pre-Tx MTV, $\Delta\text{SUV}_{\text{max}}$ and $\Delta\text{D}_{\text{mean}}$ had the strongest predictive value in evaluating treatment response for patients with cervical cancer treated with CCRT. Other imaging parameters can be replaced by these 3 parameters because of their similarities and lower predictive values. In addition, $\Delta\text{D}_{\text{min}}$ and $\Delta\text{SUV}_{\text{max}}$ have a similar value for evaluating treatment response after CCRT in cervical cancer.

1. Introduction

Cervical cancer, a type of solid tumor, is the second most commonly diagnosed cancer and the third leading cause of cancer-related death among women in developing countries [1]. For many years, cervical cancer was treated by surgery or radiotherapy alone or by a combination of these two therapies. Now, early-stage cervical cancer is treated by surgery and later-stage disease is treated by concurrent chemoradiotherapy (CCRT): the addition of chemotherapy to the standard radiotherapy regimen delays disease progression and improves patients'

survival [2–5]. Good results have been achieved in clinical treatment, but inconsistencies are evident: patients experience varying degrees of toxic side effects during CCRT [6], and some patients who receive similar standard treatments do not have similar treatment outcomes. Locoregional treatment failure was often ascribed primarily to radioresistance and led to recurrence of the disease after CCRT [7]. If reliable prognostic imaging indicators can be used to identify radioresistance early in the disease process, clinicians can adjust treatment options for patients in a timely manner.

In recent years, positron emission tomography (PET) and diffusion-

* Corresponding author at: Department of Radiology, Shengjing Hospital of China Medical University, Sanhao Street No 36, Heping District, Shenyang, Liaoning, 110004, China.

E-mail addresses: 1091899847@qq.com (C. Xu), sunhongzan@126.com (H. Sun), duziyao1215@126.com (S. Du), xinj_sjcmu@126.com (J. Xin).

<https://doi.org/10.1016/j.ejrad.2019.05.012>

Received 1 February 2019; Received in revised form 14 April 2019; Accepted 13 May 2019

0720-048X/© 2019 Elsevier B.V. All rights reserved.

weighted imaging (DWI) have been widely investigated for their values in predicting treatment response and evaluating disease progression following CCRT for uterine and cervical cancer [8–12]. As an extension of DWI, intravoxel incoherent motion magnetic resonance (IVIM MR) uses more b-values to reflect the realistic characteristics of water molecule diffusion and perfusion in tumor tissue. An IVIM model has been applied to the identification and evaluation of cervical cancer [13–15].

In this article, all imaging parameters are measured by integrated PET-MR. Integrated PET-IVIM MR scanners enable simultaneous acquisition of PET and IVIM MR imaging datasets for patients with cervical cancer who have undergone CCRT. The aim of the present study was to investigate the value of the imaging parameters and optimal combination parameters for predicting short-term treatment response in patients with cervical cancer treated with CCRT.

2. Materials and methods

2.1. Patients

From December 2017 to December 2018, we retrospectively collected data from 41 patients with cervical cancer who were treated in our hospital. The inclusion criteria were as follows: (1) all CCRT treatment options were consistent and (2) all patients with cervical cancer underwent integrated PET-MR scans 3 times. The first integrated PET-MR scan was performed within 3 days prior to CCRT, and the second scan was performed at the end of the third week of CCRT; and the third scan was performed within 1 month after CCRT.

2.2. Concurrent chemoradiotherapy

All patients were treated with a combination of external beam radiotherapy (EBRT) and high dose-rate (HDR) intracavitary brachytherapy (ICBT) by pelvic 3-D conformal external beam radiotherapy. EBRT was delivered to the whole pelvis with 6 MV photon beams at a distance of 100 cm; a daily dose of 2.0 Gy was delivered 5 times weekly for a total dose of 46–56 Gy. HDR ICBT was initiated after an EBRT dose of 30 Gy in 3 weeks. ICBT was performed once weekly with a 6-Gy fraction. The total dose at point A was 78–90 Gy, and the external dose at point B was 46–56 Gy. The chemotherapeutic regimen was cisplatin 30–40 mg/m² or nedaplatin 50 mg/week.

2.3. FDG-PET/MRI acquisition

Before examination, all patients fasted for at least 6 h (fasting blood glucose, < 6.6 mmol/L). In a resting state, the pelvic integrated PET-MR (Signa, GE Healthcare, Waukesha, WI, USA) was performed 60 min after intravenous administration of 240–350 MBq (depending on body weight) of fluorodeoxyglucose (18 F-FDG). This PET/MR scanner contains a 3 T MRI scanner (GE Signa 750 w) and time-of-flight PET. The MR and PET subsystems run simultaneously. PET performs attenuation correction of gamma rays by the 2-point Dixon MR imaging sequence. The 3-dimensional iterative ordered-subset expectation maximization algorithm, 3 iterations and 28 subsets, a 4-mm full-width at half maximum Gaussian filter, and a 128 × 128 image matrix were used to reconstruct imaging.

The pelvic axial scan ranged from the level of the vagina to the upper edge of the humerus. During the scan, the patient was breathing spontaneously. The parameters for pelvic axial T1-W, T2-W, sagittal T2-W, DWI, and IVIM imaging are summarized in Table 1.

In order to observe the parameters accurately and quantitatively, the dosages of injected drugs, waiting time, scanning conditions, and reconstruction parameters were consistent for the 3 repetitions of the integrated PET-MR scans for each patient.

2.4. Image analysis

All images were measured and analyzed by 2 radiologists who both have more than 10 years of experience in radiodiagnosis. Images obtained from PET-MR examination were imported into Advantage Workstation 4.6 (GE Medical System, Milwaukee, WI, USA). Imaging was analyzed by Fused-PET/MR software. MR diagnostic criteria for cervical cancer included high signal intensity lesions on T2WI, low signal intensity lesions on the apparent diffusion coefficient map, and high signal intensity lesions on the DWI with a b-value of 800 s/mm². The software automatically plotted the entire tumor area as the volume of interest (VOI). The VOIs were selected by 2 researchers to exclude cystic, fibrotic, and necrotic portions in the tumor [16]. Recording parameters were maximum standardized uptake values (SUV_{max}), metabolic tumor volume (MTV), and total lesion glycolysis (TLG) within the VOI. We conducted IVIM imaging post-processing by the IM-AgenGINE MRTtoolbox (Vusion Tech Ltd. Co., China). The relationship between the bi-exponential model signal change and the b-values were introduced by the functions: $S_b/S_0 = F \times \exp[-b \times (D^* + D)] + (1 - F) \times \exp(-b \times D)$ [17]. S_b and S_0 , respectively, represented the mean signal intensity with diffusion gradient b and without diffusion gradient [18]. D is the pure slow diffusion coefficient, D^* is the fast diffusion coefficient and, F is the perfusion-related diffusion fraction. Two researchers manually selected the largest area and the 2 adjacent slices of the tumor on the T2WI and PET images. Two researchers manually plotted the 3 slices of the region of interest (ROI) along the edge of the lesion. These ROIs were copied and drawn at the T2WI in the exact same position on the D and F maps. Recording parameters were minimum diffusion-related coefficient within these ROIs (D_{min}), mean diffusion-related coefficient within these ROIs (D_{mean}), mean perfusion-related parameter within these ROIs (F_{mean}). If no residual tumor was observed after treatment, the ROI was placed in the area where the lesion was originally located.

PET- and IVIM-derived parameters of percentage changes in the tumors were calculated by the following equation:

$$-\Delta \text{SUV}_{\max} = [\text{preTx SUV}_{\max} - \text{midTx SUV}_{\max}] / \text{preTx SUV}_{\max} \times 100 (\%).$$

$$-\Delta \text{MTV} = [\text{preTx MTV} - \text{midTx MTV}] / \text{preTx MTV} \times 100 (\%).$$

$$-\Delta \text{TLG} = [\text{preTx TLG} - \text{midTx TLG}] / \text{preTx TLG} \times 100 (\%).$$

$$-\Delta D_{\text{mean}} = [\text{midTx } D_{\text{mean}} - \text{preTx } D_{\text{mean}}] / \text{preTx } D_{\text{mean}} \times 100 (\%).$$

$$-\Delta D_{\text{min}} = [\text{midTx } D_{\text{min}} - \text{preTx } D_{\text{min}}] / \text{preTx } D_{\text{min}} \times 100 (\%).$$

$$-\Delta F_{\text{mean}} = [\text{midTx } F_{\text{mean}} - \text{preTx } F_{\text{mean}}] / \text{preTx } F_{\text{mean}} \times 100 (\%).$$

preTx = pre-therapy, midTx = mid-therapy (at the end of the third week)

2.5. Treatment outcome analysis

The post-therapy (PostTx) CCRT PET-MR scans were used to classify patient responses to treatment as complete metabolic responders (CMR) or non-complete metabolic responders (N-CMR) according to the European Organization for Research and Treatment of Cancer (EORTC) criteria [19]. Detailed cases of CMR and N-CMR are shown in Figs. 1 and 2.

2.6. Statistical analysis

Statistical analyses were performed with MedCalc and SPSS statistical software. To compare the CMR and N-CMR groups, we used analysis of variance and the chi-square test to compare differences in age and differences in International Federation of Gynecology and Obstetrics (FIGO) stage and tumor grade, respectively. The t -test was

Table 1

The parameters for pelvic axial T1-W, T2-W, sagittal T2-W, DWI, and IVIM imaging.

	Axial T1	Axial T2	Sagittal T2	DWI	Axial IVIM
TR	500 ms	498ms	4323ms	4000ms	6900ms
TE	8ms	79ms	65ms	238ms	minimum
Thickness	6.0mm	6.0mm	6.0mm	6.0mm	8.0mm
Interval	2.0mm	2.0mm	1.2mm	2.0mm	9.0mm
FOV	26cm	36cm	24cm	40cm	40cm
matrix size	384 × 384	384 × 384	384 × 384	128 × 128	128 × 128
NEX	2	1.5	4	6	6
b-values(s/mm ²)				0、800	0,10, 25, 50, 75,100,125,150, 200, 300, 400, 600, 800, and 1000

TR : repetition time ; TE : echo time ; FOV : Field of view ; NEX :number of excitation.

used to compare differences in PET- and IVIM-derived parameters (quantitative data with a normal distribution); otherwise, the Mann-Whitney *U* test was used. The relationships between PET- and IVIM-derived parameters and treatment responses after CCRT were analyzed by receiver operating characteristic (ROC) curves. ROC curves were compared by the DeLong test. A multiple-parameter combination prediction model was constructed using multivariate logistic regression. The optimal cutoff threshold values were determined to be the point on the ROC curve where sensitivity and specificity were maximal. The correlations between PET and IVIM parameters and percentage changes during CCRT were investigated by the Spearman rank correlation. For all of the above analyses, a 2-sided P-value of less than 0.05 denoted a significant difference.

3. Results

The clinical characteristics of the patients are summarized in

Table 2. All 41 patients completed the prescribed treatment regimen and examinations. In all, 13 (31.7%) patients were defined as N-CMR. There were no statistically significant differences in age ($p = 0.43$), FIGO stage ($p = 0.329$), or tumor grade ($p = 0.836$) between the CMR and N-CMR groups.

3.1. Univariate analyses of PET- and IVIM-derived parameters with treatment response

PET- and IVIM-derived parameters in patients in both the CMR group and the N-CMR group before and during CCRT are summarized in **Table 3.** Significant differences were detected between the CMR group and the N-CMR group in midTx D_{min} (t -test, $P = 0.025$), midTx F (t -test, $P = 0.017$), midTx MTV (U test, $P = 0.045$), ΔF (t -test, $P = 0.038$), ΔSUV_{max} (t -test, $P = 0.038$), preTx MTV (U test, $P = 0.009$).

The ROC analysis showed that several PET- and IVIM-derived parameters had a positive effect on predicting treatment response in

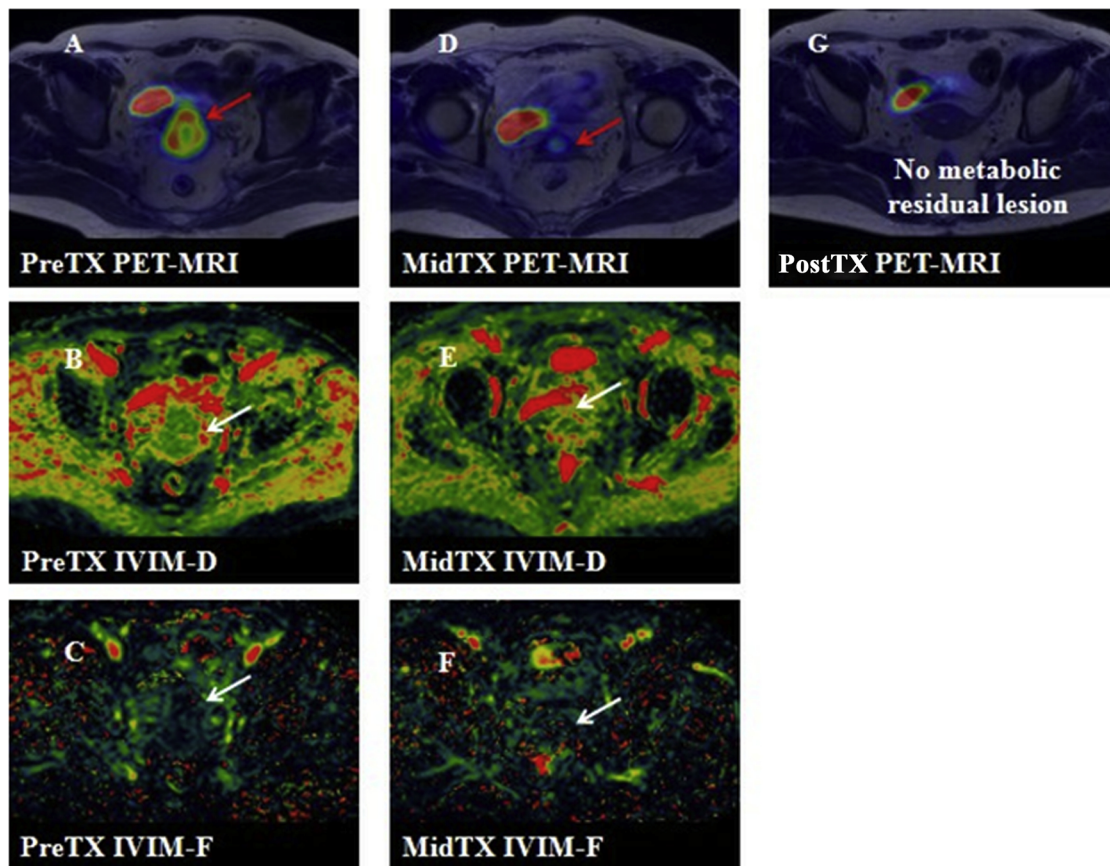


Fig. 1. Female, 65 years old, FIGO 2b stage, pathologically confirmed moderately differentiated squamous cell carcinoma ; A, B, C is T2 and PET fusion, D value, F value image before treatment ; D, E, F is T2 and PET Fusion, D-value, F-value images during treatment (at the end of the third week) ; G is T2 and PET Fusion after treatment. No metabolic residual lesion was observed one month after CCRT. Treatment response of the patient was defined as CMR group.

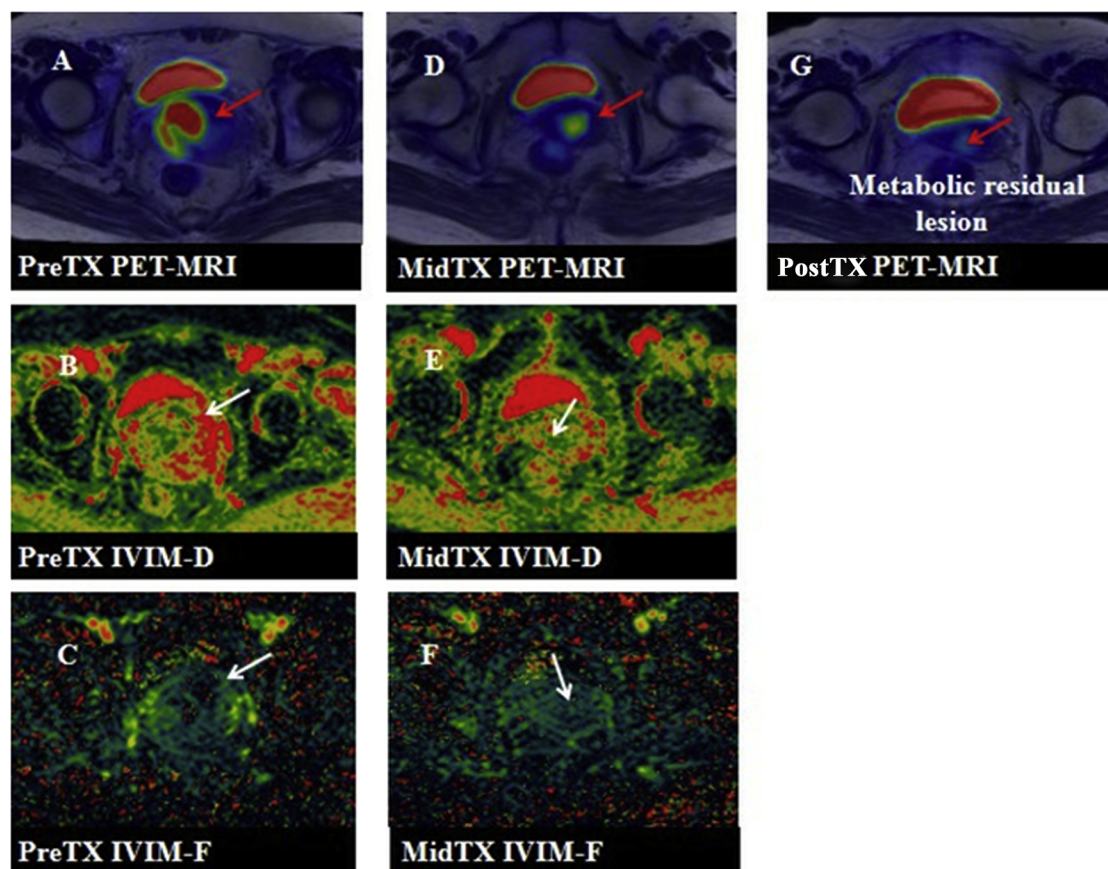


Fig. 2. Female, 66 years old, FIGO 2b stage, pathologically confirmed moderately differentiated squamous cell carcinoma ; A, B, C is T2 and PET fusion, D value, F value imaging before treatment ; D,E,F is T2 and PET Fusion, D-value, F-value imaging during treatment (at the end of the third week) ; G is T2 and PET Fusion imaging after treatment. Metabolic residual lesion was observed one month after CCRT. Treatment response of the patient was defined as N-CMR group.

Table 2
Patient characteristics.

Clinical features	Value
No. of patients	41
Mean age (range)	49.8 years(32-66)
FIGO stage:	
II	18(43.9%)
III	20(48.8%)
IV	3 (7.3%)
Tumor grade :	
Well differentiated	5(12.2%)
Moderately differentiated	19(46.3%)
Poorly differentiated	17(41.5%)
short-term outcome	
CMR	28(68.3%)
N-CMR	13(31.7%)

FIGO: The International Federation of Gynecology and Obstetrics.

patients with cervical cancer after CCRT.

Before treatment, MTV and TLG values were valuable parameters (Fig. 3).

At the end of the third week of treatment, all imaging parameters were valuable (Fig. 4).

SUV_{max} and D_{min} percentage changes during CCRT were also significant parameters (Fig. 5).

3.2. Combination analysis of PET- and IVIM-derived parameters with treatment response

A stepwise method was used to construct the multivariate logistic regression mode. $P < 0.05$ was selected to enter variable and $P > 0.05$

was fixed to remove variable. Treatment response was used as dependent variable and all imaging parameters were independent variables. Of all imaging parameters in the multivariate logistic regression analysis, the combination of preTx MTV, ΔSUV_{max} , and ΔD_{mean} had the strongest predictive potential. Other imaging parameters can be replaced by these 3 parameters because of their similarities and lower predictive values. A combination ROC of preTx MTV with ΔSUV_{max} and ΔD_{mean} expression was 0.912 ($P < 0.01$, 95% confidence interval 0.781–0.978) (Fig. 6). Multivariate logistic regression parameters are summarized in Table 4.

3.3. The correlations between PET- and IVIM-derived parameters and percentage changes during CCRT

ΔD_{min} was correlated with ΔSUV_{max} (Spearman correlation coefficient, $R = 0.338$; $P = 0.031$; $N = 41$).

4. Discussion

In this study, we aimed to evaluate treatment responses of patients with cervical cancer who had undergone CCRT using integrated multi-parameters of PET-IVIM MR imaging. In recent years, several studies have evaluated the long-term prognostic value of imaging indicators for patients with cervical cancer who have undergone CCRT [8–12,15]. The long-term outcomes of treatment are influenced by the living environment, other systemic diseases, and accidents, as well as psychological and physiological factors of patients with cervical cancer. The accuracy of individualized treatment regimens based on imaging indicators that assess long-term outcomes will also be lower than those based on short-term treatment responses. In addition, an important

Table 3
PET and IVIM derived parameters in patients with CMR group and N-CMR group before and during CCRT.

		All patients	CMR	N-CMR
D_{\min}	preTx ($\times 10^{-3}$ mm ² /s)	0.63 \pm 0.1	0.64 \pm 0.09	0.62 \pm 0.13
	midTx ($\times 10^{-3}$ mm ² /s)	0.82 \pm 0.16	0.85 \pm 0.15	0.73 \pm 0.17
	Percentage change (%)	30.13 \pm 20.44	34.43 \pm 15.45	19.72 \pm 27.28
D_{mean}	preTx ($\times 10^{-3}$ mm ² /s)	0.94 \pm 0.13	0.94 \pm 0.12	0.95 \pm 0.17
	midTx ($\times 10^{-3}$ mm ² /s)	1.19 \pm 0.21	1.23 \pm 0.19	1.09 \pm 0.22
	Percentage change (%)	27.72 \pm 23.57	32.1 \pm 21.4	17.14 \pm 26.12
F_{mean}	preTx (%)	12.49 \pm 3.68	12.82 \pm 3.63	11.69 \pm 3.84
	midTx (%)	17.25 \pm 4.7	18.36 \pm 4.4	14.57 \pm 4.48
	Percentage change (%)	41.91 \pm 28.56	47.81 \pm 27.11	27.63 \pm 27.94
SUV_{max}	preTx	13.6 \pm 7.6	13.6 \pm 7.2	13.8 \pm 8.7
	midTx	7.5 \pm 5.5	6.6 \pm 4.2	9.3 \pm 7.6
	Percentage change (%)	43.1 \pm 26.8	50.0 \pm 20.7	26.4 \pm 33.1
MTV	preTx (cm ³)	39.56 \pm 25.08	32.89 \pm 21.65	55.68 \pm 26.34
	midTx(cm ³)	21.2 \pm 18.7	16.78 \pm 13.06	31.9 \pm 25.7
	Percentage change (%)	42.1 \pm 31.52	44.82 \pm 27.63	35.55 \pm 40.05
TLG	preTx	372.07 \pm 375.22	289.58 \pm 293.2	571.4 \pm 481.52
	midTx	130.5 \pm 198.77	90.47 \pm 122.67	227.24 \pm 301.56
	Percentage change (%)	63.02 \pm 30.51	69.48 \pm 18.04	47.39 \pm 46.68

Note: Data are means \pm standard deviations. preTx = before treatment, midTx = during treatment (at the end of the third week).

indicator for predicting disease progression for cervical cancer patients treated with CCRT is treatment response after CCRT [20–22]. If the treatment response could be predicted or assessed before or during treatment, the treatment regimen which may include steps such as strengthening the dose of radiotherapy, changing the chemotherapy regimen, and evaluating the possibility of surgical treatment can be adjusted and individualized.

A large number of studies suggested that preTx MTV and preTx TLG could provide important information for evaluating prognosis for patients with cervical cancer [23–26] which was similar to our results. MTV represents the metabolic region of tumor cells and TLG is a more effective parameter that takes into account both tumor volume and metabolic activity. Our study suggested that MTV and TLG values before CCRT were important factors to predict treatment response of cervical cancer.

The time point we chose for midTx PET-MR scanning was the end of the third week of treatment, before the high-dose ICBT. Hatano believed that treatment response could be predicted at 30 Gy in radiotherapy [27]. Lin believed that a 50% reduction in physiological tumor volume in patients with cervical cancer occurred approximately 20 days after treatment [28]. Still, no consensus was reached regarding the optimal time point for scans to achieve the most accurate tumor response assessment. Our results showed that all imaging parameters were valuable for assessing treatment response at the end of the third week of treatment. According to our current and previous results, the midTx scanning time point we chose was reasonable and effective.

Lee and Heerim Nam believed tumor volume reduction on PET/computed tomography (CT) and MR images could evaluate tumor response during CCRT [29,30]. This was not consistent with our results. However, the changes in tumor morphology lag behind the death of tumor cells, and disease control with chemotherapeutic agents is, to some extent, reflected in prolonged survival. Therefore, tumor volume change after treatment lags behind physiological or even metabolic change, especially the extreme value changes which functional imaging parameters can provide. Our results showed that ΔSUV_{max} and ΔD_{\min} had the potential to evaluate treatment response. SUV_{max} represents the highest metabolic region of tumor cells. D_{\min} represents the lowest diffusion region of tumor cells. Although these two imaging parameters reflect different aspects of tumor biology, they may have similar quantitative changes during CCRT for patients with cervical cancer.

We have investigated the correlations between PET and IVIM parameters in our previous study [31]. In this current study, we further explored the correlations between the two functional imaging parameters and their percentage changes during treatment. Our results showed that ΔSUV_{max} and ΔD_{\min} had a weakly strong degree of correlation. Previous studies have indicated that ΔSUV_{max} not only is an early sensitive imaging parameter for predicting tumor response, but also a parameter for long-term prognosis, and guiding treatment [9,11]. However, PET is an invasive and expensive scan. To some extent, ΔD_{\min} may replace the roles of ΔSUV_{max} in assessing treatment response and prognosis due to its noninvasive and cheaper scan.

In previous studies, researchers only investigated the individual

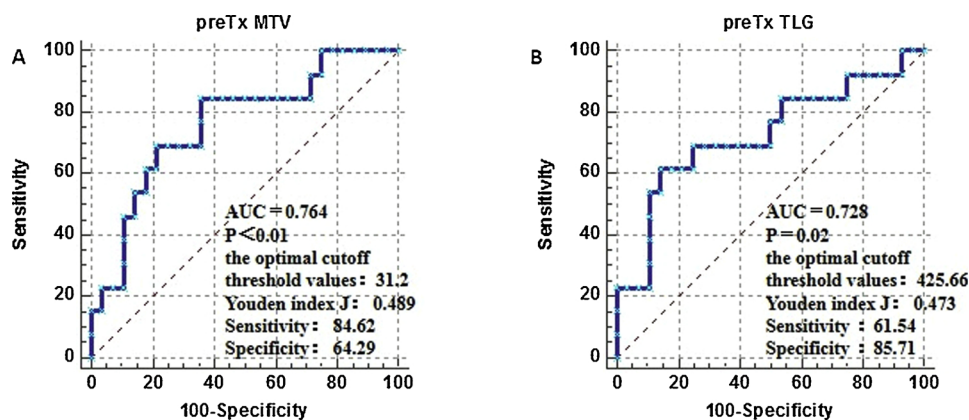


Fig. 3. preTx MTV (95% Confidence interval 0.605–0.882): MTV value before treatment; preTx TLG (95% Confidence interval 0.605–0.882): TLG value before treatment.

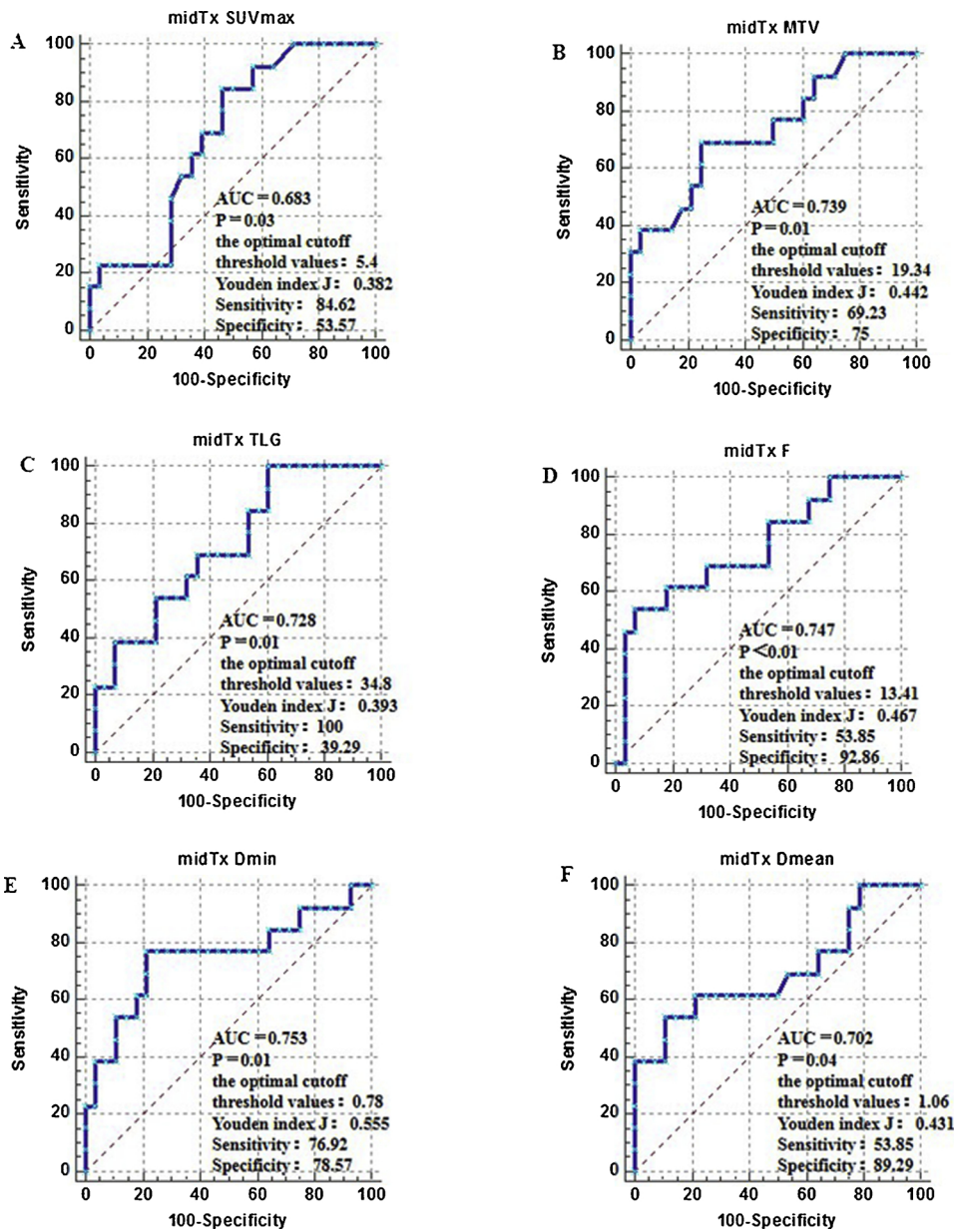


Fig. 4. midTx SUV_{max} (95% Confidence interval 0.519–0.819): SUV_{max} value during treatment. midTx MTV(95% Confidence interval 0.578–0.863): MTV value during treatment. midTx TLG(95% Confidence interval 0.567–0.855): TLG value during treatment. midTx F(95% Confidence interval 0.587–0.870): F value during treatment. midTx D_{min} (95% Confidence interval 0.593–0.874): D_{min} value during treatment. midTx D_{mean} (95% Confidence interval 0.539–0.834): D_{mean} value during treatment.

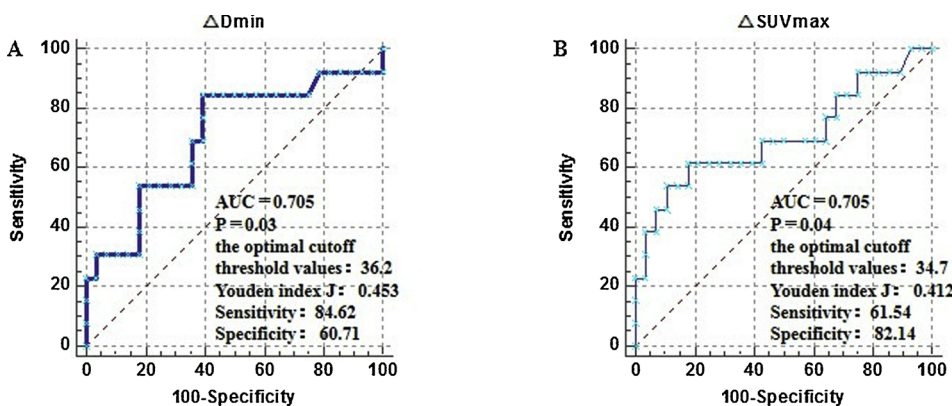


Fig. 5. ΔSUV_{max} (95% Confidence interval 0.542–0.837): SUV_{max} of percentage changes during CCRT. ΔD_{min} (95% Confidence interval 0.542–0.837): D_{min} of percentage changes during CCRT.

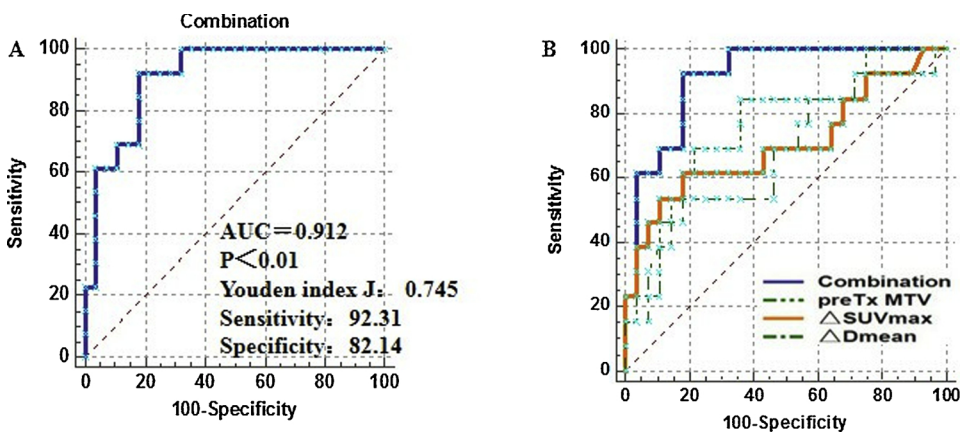


Fig. 6. PreTx MTV, Δ SUV_{max} and Δ D_{mean} combination prediction(95% Confidence interval 0.781–0.978) was better than PreTx MTV (Z = 1.964, P = 0.0495), Δ SUV_{max} (Z = 2.054, P = 0.04) or Δ D_{mean} (Z = 2.502, P = 0.0124) alone.

predictive value of imaging parameters. They believed PET-MR had a great potential for cervical cancer staging and assessment of treatment response [33–36]. In this article, we explored PET- and IVIM-derived parameters in combination to evaluate treatment responses in patients with cervical cancer treated with CCRT. All imaging parameters were measured by integrated PET-MR scanner, which enables real-time fusion of both PET and IVIM functional imaging. Integrated PET-MR can avoid movement of patients between PET and MR scans and reduce the error caused by manual correction of images; it also reduces the potential changes in the physiological function of tumor tissue due to the time interval between PET and MR examinations [32]. Therefore, integrated PET-MR can evaluate treatment response and the correlations among imaging parameters.

In our study, the combination of preTx MTV, Δ SUV_{max}, and Δ D_{mean} had the strongest predictive value. PreTx MTV and Δ SUV_{max} were both accurate imaging indexes for evaluating treatment responses separately. Δ D_{mean} cannot evaluate treatment responses individually. PreTx MTV, a pre-treatment imaging parameter, can quantify the overall initial tumor burden. SUV_{max} is the most common indicator of glucose metabolism. The D value is mainly determined by the cell density and extracellular matrix components in the tissue and is inversely related to the degree of tissue cell looseness and nucleoplasmic ratio. The Δ D_{mean} and Δ SUV_{max} reflect sensitivity to treatment

through changes in water diffusion and glucose metabolism during treatment. The three parameters may provide additional value and complement each other when evaluating treatment response, and their combination can provide more accurate evaluation. In clinical practice, the combination of these three parameters can guide the doctor to personalized patient treatment plan.

Our study has some limitations. First, the sample size was not large: more cases are needed to confirm our results. Second, all of the patients in our study had a type of squamous cell cancer. Multiple types of carcinoma should be thoroughly studied in the future. Third, early-stage cervical cancer with high SUV_{peak} may have more invasive behavior [37], but our scan range did not relate to the liver, so we could not accurately measure SUV_{peak} in this study. Finally, D* map was not in the scope of our research, and the previous preliminary study concluded that it had no predictive value [15].

5. Conclusions

Integrated PET/MR is a highly accurate multi-parameter imaging modality and should be recommended widely for evaluating treatment response in patients with cervical cancer treated with CCRT. The combination of preTx MTV, Δ D_{mean} and Δ SUV_{max} had the strongest predictive value in evaluating treatment response for patients with cervical

Table 4
Multivariate logistic regression parameters.

A. Coefficients and Standard Errors				
Variable	coefficients	Std Error	Wald	P
Δ D _{mean}	-0.090815	0.043450	4.3684	0.0366
Δ SUV _{max}	-0.096549	0.042481	5.1653	0.023
PreTx MTV	0.078899	0.031403	6.3127	0.012
Constant	2.0326			
B. Odds Ratios and Confidence Intervals				
Variable	Odds Ratio	95% CI		
Δ D _{mean}	0.9123	0.8396 to 0.9944		
Δ SUV _{max}	0.908	0.8354 to 0.9868		
PreTx MTV	1.0821	1.0175 to 1.1508		
C. Overall Model Fit				
Null Model-2 Log Likelihood	51.221			
Full Model-2 Log Likelihood	28.209			
Chi-squared	23.012			
DF	3			
Significance Level	P < 0.0001			
Cox & Snell R ²	0.4295			
Nagelkerke R ²	0.6022			

carcinoma treated with CCRT. In addition, ΔD_{\min} and ΔSUV_{\max} have a slight correlation. Clinicians can personalize treatment plans on the basis of this result.

Ethics approval and informed consent

Approved by the institutional review board. Informed consent was obtained from all subjects (patients) in this study. METHODS: retrospective, diagnostic studies.

Conflict of interest

The authors declare that they have no conflicts of interest.

References

- [1] L.A. Torre, F. Bray, R.L. Siegel, J. Ferlay, J. Lortet-Tieulent, A. Jemal, Global cancer statistics, 2012, *CA Cancer J. Clin.* 65 (2015) 87–108, <https://doi.org/10.3322/caac.21262>.
- [2] B.J. Monk, K.S. Tewari, W.J. Koh, Multimodality therapy for locally advanced cervical carcinoma: state of the art and future directions, *J. Clin. Oncol.* 25 (2007) 2952–2965, <https://doi.org/10.1200/JCO.2007.10.8324>.
- [3] P.G. Rose, B.N. Bundy, E.B. Watkins, et al., Concurrent cisplatin-based radiotherapy and chemotherapy for locally advanced cervical cancer, *N. Engl. J. Med.* 340 (1999) 1144–1153, <https://doi.org/10.1056/NEJM199904153401502>.
- [4] M. Morris, P.J. Eifel, J. Lu, et al., Pelvic radiation with concurrent chemotherapy compared with pelvic and para-aortic radiation for high-risk cervical cancer, *N. Engl. J. Med.* 340 (1999) 1137–1143, <https://doi.org/10.1056/NEJM199904153401501>.
- [5] T. Yamada, S. Ishihara, M. Kawai, Y. Itoh, S. Naganawa, M. Ikeda, Analysis of late adverse events and their chronological changes after radiationtherapy for cervical cancer, *Nagoya J. Med. Sci.* 80 (2018) 487–496, <https://doi.org/10.18999/nagjms.80.4.487>.
- [6] J.A. Green, J.M. Kirwan, J.F. Tierney, et al., Survival and recurrence after concomitant chemotherapy and radiotherapy for cancer of the uterine cervix: a systematic review and meta-analysis, *Lancet* 368 (2001) 781–786, [https://doi.org/10.1016/S0140-6736\(01\)05965-7](https://doi.org/10.1016/S0140-6736(01)05965-7).
- [7] G.M. Lima, A. Matti, G. Vara, et al., Prognostic value of posttreatment 18F-FDG PET/CT and predictors of metabolic response to therapy in patients with locally advanced cervical cancer treated with concomitant chemoradiation therapy: an analysis of intensity- and volume-based PET parameters, *Eur. J. Nucl. Med. Mol. I.* 45 (2018) 2139–2146, <https://doi.org/10.1007/s00259-018-4077-1>.
- [8] J.J. Park, K.K. Chan, B.K. Park, Prediction of disease progression following concurrent chemoradiotherapy for uterine cervical cancer: value of post-treatment diffusion-weighted imaging, *Eur. Radiol.* 26 (2015) 1–8, <https://doi.org/10.1007/s00330-015-4156-7>.
- [9] J.J. Park, C.K. Kim, B.K. Park, Prognostic value of diffusion-weighted magnetic resonance imaging and 18F-fluorodeoxyglucose-positron emission tomography/computed tomography after concurrent chemoradiotherapy in uterine cervical cancer, *Radiother. Oncol.* 120 (2016) 507–511, <https://doi.org/10.1016/j.radonc.2016.02.014>.
- [10] S.M. Schreuder, R. Lensing, J. Stoker, S. Bipat, Monitoring treatment response in patients undergoing chemoradiotherapy for locally advanced uterine cervical cancer by additional diffusion-weighted imaging: a systematic review, *J. Magn. Reson. Imaging* 42 (2015) 572–594, <https://doi.org/10.1016/j.radonc.2016.02.014>.
- [11] Dongryul Oh, J.E. Lee, S.J. Huh, et al., Prognostic significance of tumor response as assessed by sequential 18F-fluorodeoxyglucose-positron emission tomography/computed tomography during concurrent chemoradiation therapy for cervical cancer, *Int. J. Radiat. Oncol. Biol. Phys.* 87 (2013) 549–554, <https://doi.org/10.1016/j.ijrobp.2013.07.009>.
- [12] J.J. Park, C.K. Kim, S.Y. Park, et al., Assessment of early response to concurrent chemoradiotherapy in cervical cancer: value of diffusion-weighted and dynamic contrast-enhanced MR imaging, *Magn. Reson. Imaging* 32 (2014) 993–1000, <https://doi.org/10.1016/j.mri.2014.05.009>.
- [13] Y. Zhou, J.Y. Liu, C.R. Liu, et al., Intravoxel incoherent motion diffusion weighted MRI of cervical cancer - correlated with tumor differentiation and perfusion, *Magn. Reson. Imaging* 34 (2016) 1050–1056, <https://doi.org/10.1016/j.mri.2016.04.009>.
- [14] E.Y.P. Lee, X. Yu, M.M.Y. Chu, et al., ChuPerfusion and diffusion characteristics of cervical cancer based on intravoxel incoherent motion MR imaging-a pilot study, *Eur. Radiol.* 24 (2014) 1506–1513, <https://doi.org/10.1007/s00330-014-3160-7>.
- [15] L. Zhu, H.H. Wang, L.J. Zhu, et al., Predictive and prognostic value of intravoxel incoherent motion (IVIM) MR imaging in patients with advanced cervical cancers undergoing concurrent chemo-radiotherapy, *Sci. Rep.-Uk.* 7 (2017) 11635, <https://doi.org/10.1038/s41598-017-11988-2>.
- [16] D.M. Koh, D.J. Collins, Diffusion-weighted MRI in the body: applications and challenges in oncology, *AJR Am. J. Roentgenol.* 188 (2007) 1622–1635, <https://doi.org/10.2214/AJR.06.1403>.
- [17] D. Le Bihan, E. Breton, D. Lallemand, M.L. Aubin, J. Vignaud, M. Laval-Jeantet, Separation of diffusion and perfusion in intravoxel incoherent motion MRI imaging, *Radiology* 168 (1988) 497–505, <https://doi.org/10.1148/radiology.168.2.3393671>.
- [18] A. Luciani, A. Vignaud, M. Cavet, et al., Liver cirrhosis: intravoxel incoherent motion MR imaging—pilot study, *Radiology* 249 (2008) 891–899, <https://doi.org/10.1148/radiol.2493080080>.
- [19] H. Young, R. Baum, U. Cremerius, et al., Measurement of clinical and subclinical tumour response using [18F]-fluorodeoxyglucose and positron emission tomography: review and 1999 EORTC recommendations, *Eur. J. Cancer* 35 (1999) 1773–1782, [https://doi.org/10.1016/S0959-8049\(99\)00229-4](https://doi.org/10.1016/S0959-8049(99)00229-4).
- [20] N. Hardt, J.R. Van Nagell, M. Hanson, E. Donaldson, J. Yoneda, Y. Maruyama, Radiation-induced tumor regression as a prognostic factor in patients with invasive cervical cancer, *Cancer* 49 (1982) 35–39, [https://doi.org/10.1002/1097-0142\(19820101\)49:1<35::AID-CNCR2820490108>3.0.CO;2-](https://doi.org/10.1002/1097-0142(19820101)49:1<35::AID-CNCR2820490108>3.0.CO;2-).
- [21] J.H. Hong, M.D. Chen, F.J. Lin, S.G. Tang, Prognostic assessment of tumor regression after external irradiation for cervical cancer, *Int. J. Radiat. Oncol. Biol. Phys.* 22 (1992) 913–917, [https://doi.org/10.1016/0360-3016\(92\)90787-1](https://doi.org/10.1016/0360-3016(92)90787-1).
- [22] A.J. Jacobs, C. Faris, C.A. Perez, M.S. Kao, A. Galakatos, H.M. Camel, Short-term persistence of carcinoma of the uterine cervix after radiation. An indicator of long-term prognosis, *Cancer* 57 (1986) 944–950, [https://doi.org/10.1002/1097-0142\(19860301\)57:5<944::AID-CNCR2820570512>3.0.CO;2](https://doi.org/10.1002/1097-0142(19860301)57:5<944::AID-CNCR2820570512>3.0.CO;2).
- [23] F.G. Herrera, T. Breuneval, J.O. Prior, J. Bourhis, M. Ozsahin, [18F]FDG-PET/CT metabolic parameters as useful prognostic factors in cervical cancer patients treated with chemo-radiotherapy, *Radiat. Oncol.* 11 (2016) 43, <https://doi.org/10.1186/s13014-016-0614-x>.
- [24] J. Yoo, J.Y. Choi, S.H. Moon, et al., Prognostic significance of volume-based metabolic parameters in uterine cervical cancer determined using 18F-fluorodeoxyglucose positron emission tomography, *Int. J. Gynecol. Cancer* 22 (2012) 1226–1233, <https://doi.org/10.1097/igc.0b013e318260a905>.
- [25] M. Miccò, H.A. Vargas, I.A. Burger, et al., Combined pre-treatment MRI and 18F-FDG PET/CT parameters as prognostic biomarkers in patients with cervical cancer, *Eur. J. Radiol.* 83 (2014) 1169–1176, <https://doi.org/10.1016/j.ejrad.2014.03.024>.
- [26] F.Y. Liu, C.H. Lai, L.Y. Yang, et al., Utility of 18F-FDG PET/CT in patients with advanced squamous cell carcinoma of the uterine cervix receiving concurrent chemoradiotherapy: a parallel study of a prospective randomized trial, *Eur. J. Nucl. Med. Mol. Imaging* 43 (2016) 1812–1823, <https://doi.org/10.1007/s00259-016-3384-7>.
- [27] K. Hatano, Y. Sekiya, H. Araki, et al., Evaluation of the therapeutic effect of radiotherapy on cervical cancer using magnetic resonance imaging, *Int. J. Radiat. Oncol. Biol. Phys.* 45 (1999) 639–644, [https://doi.org/10.1016/S0360-3016\(99\)00228-X](https://doi.org/10.1016/S0360-3016(99)00228-X).
- [28] L.L. Lin, Z. Yang, S. Mutic, T.R. Miller, P.W. Grigsby, FDG-PET imaging for the assessment of physiologic volume response during radiotherapy in cervix cancer, *Int. J. Radiat. Oncol. Biol. Phys.* 65 (2006) 177–181, <https://doi.org/10.1016/j.ijrobp.2005.12.016>.
- [29] J.E. Lee, S.J. Huh, H. Nam, S.G. Ju, Early response of patients undergoing concurrent chemoradiotherapy for cervical cancer: a comparison of PET/CT and MRI, *Ann. Nucl. Med.* 27 (2013) 37–45, <https://doi.org/10.1007/s12149-012-0659-3>.
- [30] H. Nam, W. Park, S.J. Huh, et al., The prognostic significance of tumor volume regression during radiotherapy and concurrent chemoradiotherapy for cervical cancer using MR, *Gynecol. Oncol.* 107 (2007) 320–325, <https://doi.org/10.1016/j.ygyno.2007.06.022>.
- [31] S.Y. Du, H.Z. Sun, S. Gao, et al., Relationship between F-FDG PET metabolic parameters and MRI intravoxel incoherent motion (IVIM) histogram parameters and their correlations with clinicopathological features of cervical cancer: evidence from integrated PET/MRI, *Clin. Radiol.* 74 (2018) 178–186, <https://doi.org/10.1016/j.crad.2018.11.003>.
- [32] R. Rakheja, H. Chandarana, L. DeMello, et al., Correlation between standardized uptake value and apparent diffusion coefficient of neoplastic lesions evaluated with whole-body simultaneous hybrid PET/MRI, *Am. J. Roent. Genol.* 201 (2013) 1115–1119, <https://doi.org/10.2214/AJR.13.11304>.
- [33] J. Grueneisen, B.M. Schaarschmidt, M. Heubner, et al., Integrated PET/MRI for whole-body staging of patients with primary cervical cancer: preliminary results, *Eur. J. Nucl. Med. Mol. I.* 42 (2015) 1814–1824, <https://doi.org/10.1007/s00259-015-3131-5>.
- [34] S. Theresia, B.M. Schaarschmidt, A. Wetter, et al., Comparison of F-FDG PET/MRI and MRI for pre-therapeutic tumor staging of patients with primary cancer of the uterine cervix, *Eur. J. Nucl. Med. Mol. I.* 45 (2018) 67–76, <https://doi.org/10.1007/s00259-017-3809-y>.
- [35] M. Daniel, P. Andrzejewski, A. Sturdza, et al., Impact of hybrid PET/MR technology on multiparametric imaging and treatment response assessment of cervix cancer, *Radiother. Oncol.* 125 (2017) 420–425, <https://doi.org/10.1016/j.radonc.2017.10.036>.
- [36] T. Sarabhai, A. Tschischka, V. Stebner, et al., Simultaneous multiparametric PET/MRI for the assessment of therapeutic response to chemotherapy or concurrent chemoradiotherapy of cervical cancer patients: preliminary results, *Clin. Imag.* 49 (2018) 163–168, <https://doi.org/10.1016/j.clinimag.2018.03.009>.
- [37] L. Zhang, H.Z. Sun, S.Y. Du, W.N. Xu, J. Xin, Q.Y. Guo, Evaluation of 18F-FDG PET/CT parameters for reflection of aggressiveness and prediction of prognosis in early-stage cervical cancer, *Nucl. Med. Commun.* 39 (2018) 1045–1052, <https://doi.org/10.1097/MNM.0000000000000909>.